




## Oscillatory instabilities in three-dimensional frictional granular matter

Silvia Bonfanti <sup>1</sup>, Joyjit Chattoraj,<sup>2,3</sup> Roberto Guerra <sup>1</sup>, Itamar Procaccia,<sup>4</sup> and Stefano Zapperi <sup>1,5</sup>

<sup>1</sup>*Center for Complexity and Biosystems, Department of Physics, University of Milan, via Celoria 16, 20133 Milan, Italy*

<sup>2</sup>*School of Physical and Mathematical Sciences, Nanyang Technological University, Singapore*

<sup>3</sup>*Institute of High Performance Computing, Agency for Science, Technology and Research, Singapore*

<sup>4</sup>*Department of Chemical Physics, Weizmann Institute of Science, Rehovot 76100, Israel*

<sup>5</sup>*CNR—Consiglio Nazionale delle Ricerche, Istituto di Chimica della Materia Condensata e di Tecnologie per l'Energia, Via R. Cozzi 53, 20125 Milan, Italy*



(Received 12 September 2019; revised manuscript received 22 November 2019; accepted 29 March 2020; published 4 May 2020)

The dynamics of amorphous granular matter with frictional interactions cannot be derived in general from a Hamiltonian and therefore displays oscillatory instabilities stemming from the onset of complex eigenvalues in the stability matrix. These instabilities were discovered in the context of one- and two-dimensional systems, while the three-dimensional case was never studied in detail. Here we fill this gap by deriving and demonstrating the presence of oscillatory instabilities in a three-dimensional granular packing. We study binary assemblies of spheres of two sizes interacting via classical Hertz and Mindlin force laws for the longitudinal and tangent interactions, respectively. We formulate analytically the stability matrix in three dimensions and observe that a couple of complex eigenvalues emerge at the onset of the instability as in the case of frictional disks in two dimensions. The dynamics then shows oscillatory exponential growth in the mean-square displacement, followed by a catastrophic event in which macroscopic portions of mechanical stress and energy are lost. The generality of these results for any choice of forces that break the symplectic Hamiltonian symmetry is discussed.

DOI: [10.1103/PhysRevE.101.052902](https://doi.org/10.1103/PhysRevE.101.052902)

### I. INTRODUCTION

The mechanics of dense granular matter has attracted wide interest for decades as a paradigmatic example of disordered glassy systems [1–4] and for its importance for technological applications in several fields, from pharmaceuticals to agriculture [5]. In contrast with other disordered materials, such as silica glasses or metallic glasses where a standard atomistic description is in principle possible, granular media are ruled by *mesoscale* frictional interactions between grains. As a consequence of this, frictional granular materials cannot be described by a Hamiltonian from which the intergranule forces can be derived. The fundamental reason for this is that frictional forces depend on time and velocities, and can thus not be incorporated into a Hamiltonian. It was discovered and demonstrated recently that the lack of a Hamiltonian has generic consequences for the dynamics of granular media in the form of oscillatory instabilities that can drive the system to catastrophic mechanical failure [6–8].

Since the dynamics of granular media is not derivable from a Hamiltonian, the usual approach to the stability of amorphous systems, which is based on the analysis of the Hessian matrix (second derivative of the Hamiltonian with respect to coordinates), is not tenable. Nevertheless, forces exist, and the dynamics follows Newton's equations for the accelerations in terms of these forces. The stability of a stationary solution of these equations is determined by the so-called “*J*-matrix,” which is the first derivative of the forces with respect to the coordinates; cf. Sec. II below. The formalism that exposes the instability and its consequences were explored so far only

in two dimensions [6,7]. In the present paper, we extend the formulation to three dimensions, compute analytically the *J*-matrix for assemblies of compressed frictional spheres subject to external shear forces, and demonstrate the instability and its consequences.

The structure of this paper is as follows: in Sec. II we describe the generalization of the model studied in Refs. [6,7] to three dimensions. The force between spheres and the equations of motion are described. In Sec. III we discuss the numerical protocols used to expose the oscillatory instability. Section IV describes the results of the numerical simulations and the catastrophic failure that results from the instability. The last section, Sec. V, offers a summary and some concluding remarks.

### II. MODEL AND EQUATIONS OF MOTION

#### A. Forces

To study the oscillatory instability we employ here a generalization to three dimensions of the same model used before in two dimensions. There is nothing special about this model except that it is time-honored, being used many times by many authors. We have checked explicitly that changing the analytic forms of the interaction forces, for example, changing the longitudinal force to be simply linear in the tangential displacement, does not affect that appearance of the instability. The point is that the crucial ingredient is that the forces are not derivable from a Hamiltonian, and the rest follows quite generically.

The model discussed here consists of a binary mixture of  $N = 100$  frictional spheres of mass  $m$  in a box of size  $L^3$ , half of which with radius  $\sigma_1 = 0.5$  and the other half with  $\sigma_2 = 0.7$ . The position of the center of mass of the  $i$ th sphere is denoted  $\mathbf{r}_i$ . The interaction between two spheres has a normal and a tangential component. When the assembly of spheres is compressed the spheres overlap. The normal force between the  $i$ th and the  $j$ th spheres is determined by the amount of overlap  $\delta_{ij} \equiv \sigma_i + \sigma_j - r_{ij}$ , where  $\mathbf{r}_{ij} \equiv \mathbf{r}_i - \mathbf{r}_j$ . We choose for the normal force the Hertzian model, but stress that the qualitative nature of our results is independent of the precise choice of the forces:

$$\mathbf{F}_{ij}^{(n)} = k_n \delta_{ij}^{3/2} \hat{\mathbf{r}}_{ij}, \quad \hat{\mathbf{r}}_{ij} \equiv \mathbf{r}_{ij} / r_{ij}. \quad (1)$$

The tangential force is caused by the tangential displacement  $\mathbf{t}_{ij}$  between adjacent spheres. The tangential force is always orthogonal to  $\hat{\mathbf{r}}_{ij}$ . Upon first contact between the particles,  $\mathbf{t}_{ij} = 0$ . In three dimensions the tangential displacement is determined by a three-dimensional (3D) angular coordinate  $\boldsymbol{\theta}_i \equiv \{\theta_i^x, \theta_i^y, \theta_i^z\}$ . The change in tangential displacement is given by

$$d\mathbf{t}_{ij} = d\mathbf{r}_{ij} - (d\mathbf{r}_{ij} \cdot \mathbf{r}_{ij}) \hat{\mathbf{r}}_{ij} + \hat{\mathbf{r}}_{ij} \times (\sigma_i d\boldsymbol{\theta}_i + \sigma_j d\boldsymbol{\theta}_j). \quad (2)$$

Following this equation one computes  $\mathbf{t}_{ij}$  by integrating over time the relative velocity of the particles at the point of contact. In the Mindlin model, the tangential force depends on  $\mathbf{t}_{ij}$  and on the contact area which is proportional to  $\sqrt{\delta_{ij}}$  [9]:

$$\mathbf{F}_{ij}^{(t)} = -k_t \delta_{ij}^{1/2} \mathbf{t}_{ij} \hat{\mathbf{t}}_{ij}. \quad (3)$$

Like in all frictional models the tangential force is required to satisfy the Coulomb condition

$$\mathbf{F}_{ij}^{(t)} \leq \mu \mathbf{F}_{ij}^{(n)}, \quad (4)$$

where  $\mu$  is the friction coefficient. For the sake of writing an analytic form of the stability  $J$ -matrix we smooth out the Coulomb law such that the tangential force will have smooth derivatives; we choose

$$\mathbf{F}_{ij}^{(t)} = -k_t \delta_{ij}^{1/2} \left[ 1 + \frac{\mathbf{t}_{ij}}{t_{ij}^*} - \left( \frac{\mathbf{t}_{ij}}{t_{ij}^*} \right)^2 \right] \mathbf{t}_{ij} \hat{\mathbf{t}}_{ij}, \quad (5)$$

$$t_{ij}^* \equiv \mu \frac{k_n}{k_t} \delta_{ij}.$$

The derivative of the force with respect to  $\mathbf{t}_{ij}$  vanishes smoothly at  $\mathbf{t}_{ij} = \mathbf{t}_{ij}^*$ , and the Coulomb law (4) is fulfilled. We stress that the instabilities reported below do not depend on this smoothing of the tangential force; instabilities are often seen before any Coulomb limit is reached.

### B. Equations of motion

Once we defined the forces we can write the equations of motion, which are simply Newton's equations for an extended set of coordinates  $\mathbf{q}_i = \{\mathbf{r}_i, \boldsymbol{\theta}_i\}$ :

$$m \frac{d^2 \mathbf{r}_i}{dt^2} = \mathbf{F}_i(\mathbf{q}_1, \mathbf{q}_2, \dots, \mathbf{q}_N),$$

$$I_i \frac{d^2 \boldsymbol{\theta}_i}{dt^2} = \mathbf{T}_i(\mathbf{q}_1, \mathbf{q}_2, \dots, \mathbf{q}_N), \quad (6)$$

where  $I_i$  are moments of inertia for the spheres,  $\mathbf{F}_i$  are forces, and  $\mathbf{T}_i$  are torques.

In the simulations reported below we employ a unit mass  $m_i = 1$  and moment of inertia  $I_i = 0.4m_i\sigma_i^2$ . The normal interaction between the granular particles is given by Eq. (1), while the tangential one is given by Eq. (5), with  $k_n = 200\,000$  and  $k_t = 2k_n/7$ . We use  $m$ ,  $2\sigma_1$ , and  $\sqrt{m(2\sigma_1)^{-1/2}k_n^{-1}}$  as units of mass, length, and time, respectively. We fix the friction coefficient to a high value,  $\mu = 10$ , to emphasize that the existence of a Coulomb threshold is not responsible for the reported phenomenology.

### C. The stability matrix

Using the smoothed-out force (5) allows us to compute analytically the stability matrix, which is an operator obtained from the derivatives of the force  $\mathbf{F}_i$  and the torque  $\mathbf{T}_i$  on each particle with respect to the coordinates. In other words,

$$J_{ij}^{\alpha\xi} \equiv \frac{\partial \tilde{F}_i^\alpha}{\partial q_j^\xi}, \quad \tilde{F}_i \equiv \sum_j \tilde{\mathbf{F}}_{ij}, \quad (7)$$

where  $\mathbf{q}_j$  stands for either a spatial position or a tangential coordinate, and  $\tilde{\mathbf{F}}_i$  stands for either a force or a torque. We stress the obvious fact that  $\mathbf{J}$  is not a symmetric operator. Being real it can possess pairs of complex eigenvalues. When these appear, the system will exhibit oscillatory instabilities, since one of each complex pair will cause an oscillatory exponential divergence of any perturbation, and the other an oscillatory exponential decay. The actual calculation of the operator  $\mathbf{J}$  for the 3D case is detailed in Appendix A.

## III. SIMULATION PROTOCOLS AND THE BIRTH OF THE INSTABILITY

The equations of motion are solved using two types of algorithms: ‘‘Newtonian’’ and ‘‘overdamped.’’ The first is simply a solution of the Newton equations of motion with the given forces (6). The second algorithm is solving the same equations of motion but with a damping force that is proportional to the velocities of the centers of mass  $\dot{\mathbf{r}}_i$  of the spheres with a coefficient of proportionality  $\eta_v = m\eta_0$ . If not otherwise mentioned we use  $\eta_0 = 2.2 \times 10^{-2}$  expressed in reduced units. This value of  $\eta_0$  ensures that the dynamics is overdamped as the damping timescale  $\eta_v^{-1}$  is of the order of the time that sounds needs to travel one particle diameter. The reader should note that the overdamped equations are employed to reach a stationary solutions with zero forces  $\mathbf{F}_i$  and torques  $\mathbf{T}_i$  on all the disks for the purpose of computing the  $J$ -matrix. We use LAMMPS [10] to perform the numerical integration for these two algorithms, with integration time step  $10^{-5} \sqrt{(2\sigma_1)^{1/2} k_n m^{-1}}$ .

An initial configuration is prepared by arranging assemblies of binary spheres randomly in a 3D box and then perform two consecutive runs of overdamped dynamics to bring the configuration at mechanical equilibrium. The initial configuration is prepared focusing on a frictionless system (i.e.,  $\mu = 0$ ), and hence has no complex eigenvalues. Afterwards, we switch on friction and perform athermal quasistatic (AQS) simulations: starting from the initial stable configuration we

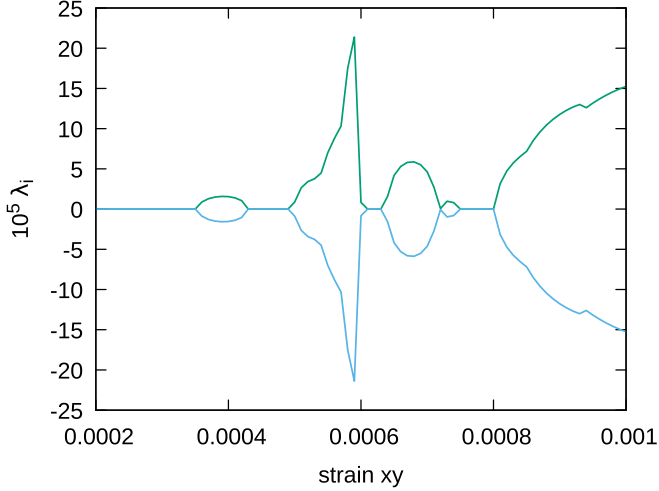


FIG. 1. Evolution of minimum (blue line) and maximum (green line) complex eigenvalue pair with increasing strain, using AQS protocol.

shear the simulation box along the ( $x$ ) direction by the amount  $\delta\gamma$ , and then we run the overdamped dynamics until the system reaches mechanical equilibrium. The system is considered to be in mechanical equilibrium when the net force on each sphere is less than  $5 \times 10^{-14}$ . After each such steps we diagonalize the  $J$ -matrix and calculate the eigenvalues. As in the two-dimensional (2D) system [6], at some value of the strain we identify the birth of a couple of conjugate complex eigenvalues.

#### A. The oscillatory instability

When a pair of complex eigenvalues  $\lambda_{1,2} = \lambda_r \pm i\lambda_i$  gets born, a novel instability mechanism develops. A pair of complex conjugate eigenvalues correspond to *four* solutions  $e^{i\omega t}$  to the linearized equation of motion with

$$i\omega_{1,2} = \omega_i \pm i\omega_r, \quad i\omega_{3,4} = -\omega_i \pm i\omega_r, \quad (8)$$

with  $\omega_r \pm i\omega_i = \sqrt{\lambda_r \pm i\lambda_i}$ . The first pair in Eq. (8) will induce an oscillatory motion with an exponential growth of any deviation  $\mathbf{q}(0)$  from a state of mechanical equilibrium,

$$\mathbf{q}(t) = \mathbf{q}(0)e^{\omega_i t} \sin(\omega_r t). \quad (9)$$

The second pair represents an exponentially decaying oscillatory solution. The actual spatial dynamics that sets in due to this instability will be discussed below in Sec. IV. Figure 1 shows the imaginary component of the dominant eigenpair. Note that with increasing strain the imaginary component can reduce and disappear, then reappear as  $\gamma$  is increased further. At higher values of  $\gamma$  one can easily obtain the simultaneous existence of many complex eigenpairs.

#### IV. DYNAMICAL CONSEQUENCES OF THE INSTABILITY

Once the  $J$ -matrix exhibits at least one conjugate complex pair of eigenvalues, the system loses mechanical stability. To see the evolution under the influence of this instability one needs to run the Newtonian equations (6). Starting from a configuration with only a pair of complex eigenvalues, with

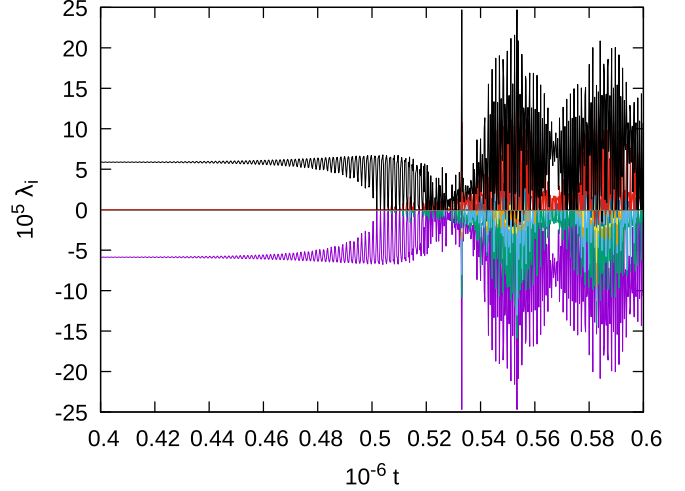


FIG. 2. Time dependence of the imaginary component of all 600 eigenvalues of the system during a Newtonian simulation.

large  $\lambda_i = 5.87 \times 10^{-5}$ , we run the Newtonian dynamics and evaluate the eigenvalues of the  $J$ -matrix at fixed intervals of time. As in the 2D case, we observe that the eigenvalues remain constant for a period of time until an instability develops; cf. Fig. 2. The complex eigenvalue induce a spiral motion in three dimensions as shown below.

To underline the exponential growth of small perturbations we consider the mean-square displacement  $M(t)$  as a function of time:

$$M(t) \equiv \frac{1}{N} \sum_i \left\{ \Delta r_i^x(t)^2 + \Delta r_i^y(t)^2 + \Delta r_i^z(t)^2 + \sigma_i^2 [\Delta \theta_i^x(t)^2 + \Delta \theta_i^y(t)^2 + \Delta \theta_i^z(t)^2] \right\}, \quad (10)$$

which is reported in Fig. 3(a). We observe an increase in time of about 10 orders of magnitude following an oscillatory exponential growth. The blue curve represents the computed MSD as a function of time, and the red dotted curve is the predicted exponential:  $a_0 \exp[2\omega_i t]$  where  $a_0$  represent an offset constant. Figure 3(b) reports a blow up of the MSD growth with the fitted function (red dotted curve) being  $a_0 \exp[2\omega_i t] [\sin(\omega_r t + \psi)]^2$  with  $\psi$  fitted. The values of fitted  $\omega_r$  and  $\omega_i$  correspond perfectly to those expected frequencies computed from the complex eigenvalue.

The particle trajectories during the development of the instability display a 3D funnel motion; see Fig. 4.

We focus finally on the virial component of the shear stress  $\sigma_{xy} = -\frac{1}{L^2} \sum_{i \neq j} r_{ij}^x F_{ij}^y$  and find that the trend reported in Fig. 5 is also similar to the 2D case. During the linear stage of the development of the instability the stress oscillates around zero, with elastic energy given to particle motion and back [Fig. 5(b)]. Once the nonlinear regime is reached the system goes through a catastrophic failure, which is induced by granules losing contacts. Then macroscopic portions of stress and energy are lost.

#### V. CONCLUSIONS

We presented the development of mechanical instabilities in a disordered packing of frictional spheres, extending to

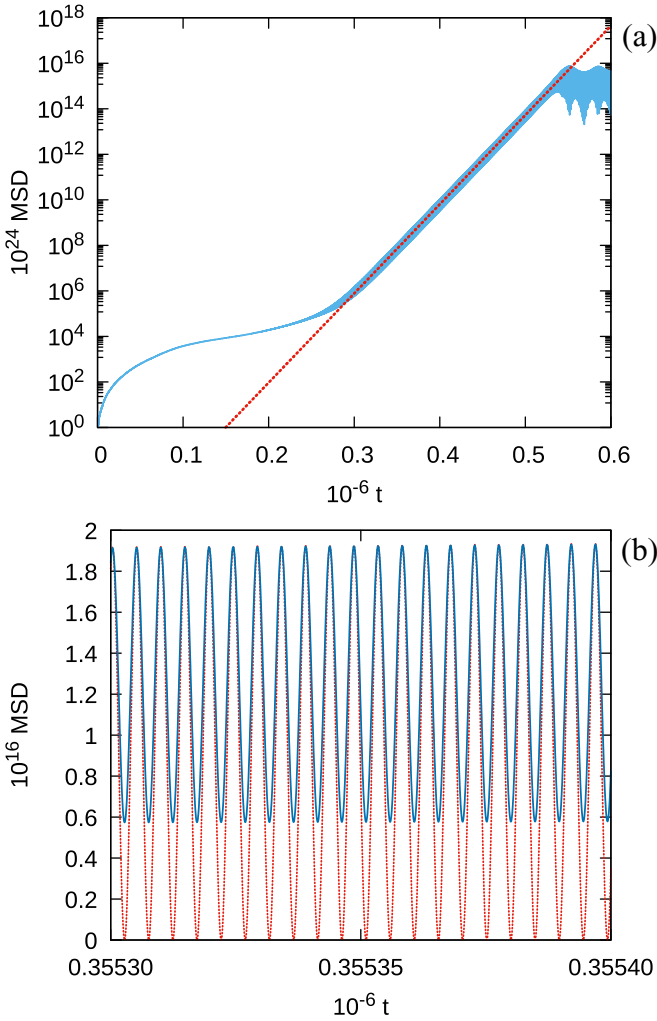


FIG. 3. MSD (blue line) and fit (red dotted line) during the Newtonian dynamics. (a) The fit is the predicted exponential growth from the linear instability,  $a_0 \exp[2\omega_1 t]$ , with  $a_0$  being fitted. (b) The MSD is fitted by the exponential oscillatory instability prediction,  $a_0 \exp[2\omega_1 t][\sin(\omega_1 t + \psi)]^2$ , with  $\psi$  fitted, as explained in the paper.

three dimensions the description of the  $J$ -matrix previously derived for 2D disks [6,7]. We have shown that there exist instabilities arising in typical granular compounds under external shear which are formally related to the emergence of imaginary eigenvalues; these dictate the characteristic time of the exponential growth and of the oscillatory period of particles motion. Importantly, these results should hold for any kind of normal and tangential force expressions which are not derivable from a Hamiltonian, thus providing a general framework to predict the shear force limit and the response of the system upon its crossing.

We would like to point out that our granular packing is prepared in a way that leads to an isotropic contact distribution. The proposed mechanism therefore describes the development of the first frictional instability at low shear, affecting the initial shear stress by a significant amount. In future work, it will be important to confirm if this instability remains macroscopically relevant also for larger strains when the contact distribution becomes more anisotropic. Previous work compared discrete element models with experimental

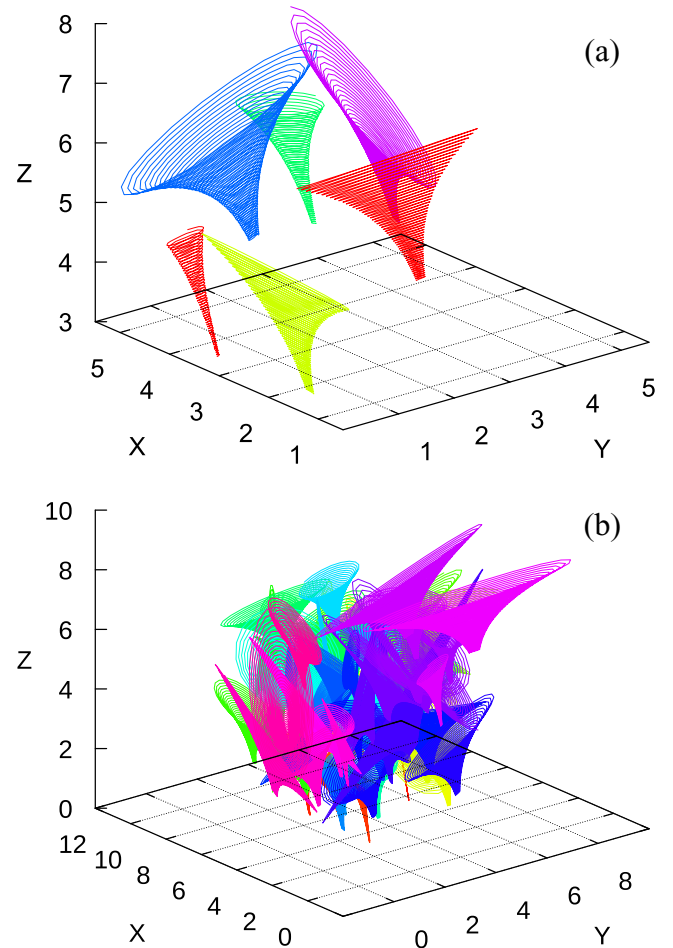


FIG. 4. Views of the trajectory of (a) few and (b) many spheres during the Newtonian dynamics. Here actual particle displacements are amplified by a factor  $10^9$ . Viewing the funnel-like trajectory from a specific perspective might resemble the view of the spirals in two dimensions.

data for granular packings in a steady-state flow regime, and a similar instability was not discussed [11]. Further work is thus needed to clarify if the mechanism we propose remains valid in the limit of large strains.

The mechanism we discuss here should describe the amplification of mechanical perturbations in countless granular matter systems extending over a large range of scales. Earthquake faults are often separated by a granular grit that is sheared by the slow motion of tectonic plates [12]. The development and growth of mechanical instabilities described here has thus a straightforward application to slip nucleation in the geophysical context [13,14]. Other relevant applications of our theoretical framework comprise the design of pharmaceutical tablets, the modeling of the formation of icebergs, or the stability of grains in silos. As long as the dynamics is describable by forces which are not derivable from a Hamiltonian, this instability should be generic.

#### ACKNOWLEDGMENTS

This work is supported by the scientific and cooperation agreement between Italy and Israel through the project COMPAMP/DISORDER, by the ISF-Singapore exchange



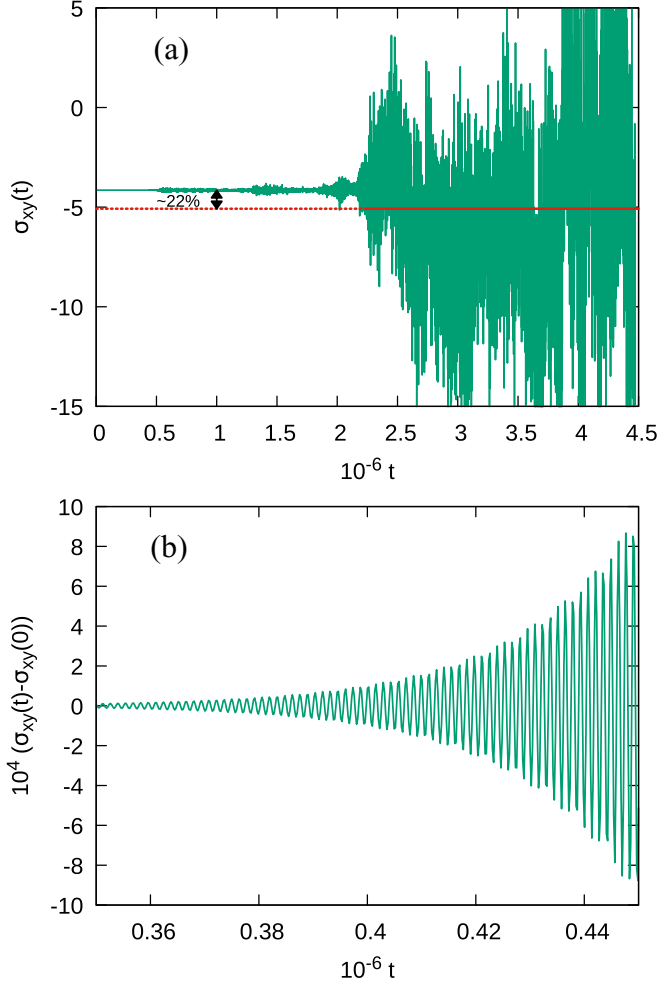


FIG. 5. (a) The long-time evolution of the shear stress (virial contribution)  $\sigma_{xy}$  versus time, during Newtonian dynamics. When the nonlinear regime is reached, the stress experiences a macroscopic drop, in the present case of 22%. (b) Enlarged view of the stress change during the linear evolution of the instability.

program, and by the US-Israel Binational Science Foundation. We thank Massimo Pica Ciamarra for his important contributions to the development of the ideas expounded in this paper.

## APPENDIX A: CALCULATION OF THE OPERATOR $\mathbf{J}$ IN THREE DIMENSIONS

The Jacobian operator  $\mathbf{J}$ , which represents the dynamical response of the system, is given by the derivative of the forces and of the torques acting on the particles with respect to all the degrees of freedom. The interaction forces used in this work are recalled in Sec. A 1, and the tangential displacement and its derivative are described in Sec. A 2. The expressions for all the components of  $\mathbf{J}$  and how these components are arranged as a matrix are reported in Appendix B.

### 1. Interaction force

In our model, a pair of granules interacts when they overlap. The overlap distance  $\delta_{ij}$  is given by

$$\delta_{ij} = \sigma_i + \sigma_j - r_{ij}, \quad (\text{A1})$$

where  $r_{ij}$  is the center-to-center distance of a pair- $i$  and  $j$ , and  $\sigma_i$  is the radius of particle  $i$ . The pair vector  $\mathbf{r}_{ij}$  is defined as

$$\mathbf{r}_{ij} = \mathbf{r}_i - \mathbf{r}_j. \quad (\text{A2})$$

The pair-interaction force  $\mathbf{F}_{ij}$  has two contributions.  $\mathbf{F}_{ij}^{(n)}$  is the force acting along the normal direction of the pair  $\hat{\mathbf{r}}_{ij}$ , and  $\mathbf{F}_{ij}^{(t)}$  is the force acting along the tangential direction of the pair  $\hat{\mathbf{t}}_{ij}$ . The normal force is Hertzian:

$$\mathbf{F}_{ij}^{(n)} = k_n \delta_{ij}^{3/2} \hat{\mathbf{r}}_{ij}, \quad (\text{A3})$$

where  $k_n$  is the force constant with dimension: force per length<sup>3/2</sup>. The tangential force  $\mathbf{F}_{ij}^{(t)}$  is a function of both the overlap distance  $\delta_{ij}$  and the tangential displacement  $t_{ij}$ . As done in previous work for a 2D frictional system, we have modified the standard expression for  $\mathbf{F}_{ij}^{(t)}$  and included a few higher-order terms of  $t_{ij}$  (i.e.,  $|t_{ij}|$ ) such that the derivative of the force function  $F_{ij}^{(t)}$  with respect to tangential distance  $t_{ij}$  becomes continuous and it goes to zero smoothly. We use the following form:

$$\begin{aligned} \mathbf{F}_{ij}^{(t)} &= -k_t \delta_{ij}^{1/2} \left[ 1 + \frac{t_{ij}}{t_{ij}^*} - \left( \frac{t_{ij}}{t_{ij}^*} \right)^2 \right] t_{ij} \hat{\mathbf{t}}_{ij} \\ &= -k_t \delta_{ij}^{1/2} t_{ij}^* \hat{\mathbf{t}}_{ij}, \quad \text{if } k_t \delta_{ij}^{1/2} t_{ij} > \mu |\mathbf{F}_{ij}^{(n)}|, \end{aligned} \quad (\text{A4})$$

where  $k_t$  is the tangential force constant. Its dimension is force per length<sup>3/2</sup>.  $t_{ij}^*$  is the threshold tangential distance:

$$t_{ij}^* = \mu \frac{k_n}{k_t} \delta_{ij}, \quad (\text{A5})$$

where  $\mu$  is the friction coefficient, a scalar quantity, which essentially determines the maximum strength of the tangential force with respect to the normal force at a fixed overlap  $\delta_{ij}$ . The derivative of  $\mathbf{F}_{ij}^{(t)}$  with respect to  $t_{ij}$  vanishes at  $t_{ij}^*$ , as it turns out:

$$\begin{aligned} \frac{\partial \mathbf{F}_{ij}^{(t)}}{\partial t_{ij}} &= k_t \delta_{ij}^{1/2} \left[ 1 + 2 \frac{t_{ij}}{t_{ij}^*} - 3 \left( \frac{t_{ij}}{t_{ij}^*} \right)^2 \right] \\ &= 0, \quad \text{if } k_t \delta_{ij}^{1/2} t_{ij} > \mu |\mathbf{F}_{ij}^{(n)}|. \end{aligned} \quad (\text{A6})$$

We stress here that the above forces imply a non-Hamiltonian dynamics. That is, there is not a function  $U(\delta, t)$  such that  $\mathbf{F}^{(n)} = -\frac{\partial U}{\partial \delta}$  and  $\mathbf{F}^{(t)} = -\frac{\partial U}{\partial t}$ .

### 2. Tangential displacement

The tangential force is a function of both  $t_{ij}$  and  $\mathbf{r}_{ij}$ . The derivative of this force thus includes the derivative of the two latter quantities. Here we evaluate these derivatives using the chain rule.

The derivative of tangential displacement  $t_{ij}$  with respect to time  $t$  is

$$\frac{dt_{ij}}{dt} = \mathbf{v}_{ij} - \mathbf{v}_{ij}^n + \hat{\mathbf{r}}_{ij} \times (\sigma_i \boldsymbol{\omega}_i + \sigma_j \boldsymbol{\omega}_j), \quad (\text{A7})$$

where  $\mathbf{v}_{ij} = \mathbf{v}_i - \mathbf{v}_j$  is the relative velocity of pair  $i$  and  $j$ .  $\mathbf{v}_{ij}^n$  is the projection of  $\mathbf{v}_{ij}$  along the normal direction  $\hat{\mathbf{r}}_{ij}$ .  $\mathbf{v}_{ij} - \mathbf{v}_{ij}^n$  is the tangential component of the relative velocity.  $\boldsymbol{\omega}_i$  and  $\boldsymbol{\omega}_j$

are the angular velocity of  $i$  and  $j$ , respectively. In differential form, the above equation reads

$$dt_{ij} = d\mathbf{r}_{ij} - (d\mathbf{r}_{ij} \cdot \hat{\mathbf{r}}_{ij})\hat{\mathbf{r}}_{ij} + \hat{\mathbf{r}}_{ij} \times (\sigma_i d\boldsymbol{\theta}_i + \sigma_j d\boldsymbol{\theta}_j), \quad (\text{A8})$$

where  $d\boldsymbol{\theta}_i$  is the angular displacement of  $i$ , which follows the relation  $d\boldsymbol{\omega}_i = \frac{d\theta_i}{dt}$ .

Hereafter we assume the 3D system. Therefore,  $\omega_i$ , and so  $\theta_i$ , have components along  $\hat{x}$ ,  $\hat{y}$ ,  $\hat{z}$ , and the cross-product is

$$\begin{aligned} \hat{\mathbf{r}}_{ij} \times d\boldsymbol{\theta}_i = & \left( \frac{y_{ij}}{r_{ij}} d\theta_i^z - \frac{z_{ij}}{r_{ij}} d\theta_i^y \right) \hat{x} + \left( \frac{z_{ij}}{r_{ij}} d\theta_i^x - \frac{x_{ij}}{r_{ij}} d\theta_i^z \right) \hat{y} \\ & + \left( \frac{x_{ij}}{r_{ij}} d\theta_i^y - \frac{y_{ij}}{r_{ij}} d\theta_i^x \right) \hat{z}. \end{aligned} \quad (\text{A9})$$

Now, if particle  $i$  changes its position the angular displacement remains unaffected,  $\frac{d\theta_i^\alpha}{dr_i^\alpha} = 0$ . Thus, the change in tangential displacement along  $\beta$  due to the change in position of particle  $i$  along  $\alpha$  contributes only in translations, and it can be written as

$$\frac{dt_{ij}^\beta}{dr_i^\alpha} = \Delta_{\alpha\beta} - \frac{r_i^\alpha r_{ij}^\beta}{r_{ij}^2}, \quad (\text{A10})$$

where  $\Delta_{\alpha\beta}$  is the Kronecker  $\delta$ , which is one when  $\alpha = \beta$ , or else zero. Similarly, a change in rotational coordinates does not modify the particles' relative distance,  $\frac{dr_{ij}^\beta}{d\theta_i^\alpha} = 0$ . Thus, the change in tangential displacement along  $\beta$  due to the change in  $\theta_i$  is

$$\begin{bmatrix} \frac{dt_{ij}^x}{d\theta_i^x} = 0 & \frac{dt_{ij}^x}{d\theta_i^y} = -\sigma_i \frac{z_{ij}}{r_{ij}} & \frac{dt_{ij}^x}{d\theta_i^z} = +\sigma_i \frac{y_{ij}}{r_{ij}} \\ \frac{dt_{ij}^y}{d\theta_i^x} = +\sigma_i \frac{z_{ij}}{r_{ij}} & \frac{dt_{ij}^y}{d\theta_i^y} = 0 & \frac{dt_{ij}^y}{d\theta_i^z} = -\sigma_i \frac{x_{ij}}{r_{ij}} \\ \frac{dt_{ij}^z}{d\theta_i^x} = -\sigma_i \frac{y_{ij}}{r_{ij}} & \frac{dt_{ij}^z}{d\theta_i^y} = +\sigma_i \frac{x_{ij}}{r_{ij}} & \frac{dt_{ij}^z}{d\theta_i^z} = 0 \end{bmatrix}. \quad (\text{A11})$$

The magnitude of tangential distance  $t_{ij}$  can be obtained from the relation  $t_{ij}^2 = \sum_\alpha t_{ij}^{\alpha 2}$ , and its differential follows  $dt_{ij} = \sum_\alpha \frac{t_{ij}^\alpha}{t_{ij}} dt_{ij}^\alpha$ . The derivatives of tangential distance  $t_{ij}$  with respect to  $r_i^\alpha$  and  $\theta_i^\alpha$  can be expressed as

$$\frac{dt_{ij}}{dr_i^\alpha} = \left( \frac{t_{ij}^x}{t_{ij}} \right) \frac{dt_{ij}^x}{dr_i^\alpha} + \left( \frac{t_{ij}^y}{t_{ij}} \right) \frac{dt_{ij}^y}{dr_i^\alpha} + \left( \frac{t_{ij}^z}{t_{ij}} \right) \frac{dt_{ij}^z}{dr_i^\alpha}, \quad (\text{A12})$$

$$\frac{dt_{ij}}{d\theta_i^\alpha} = \left( \frac{t_{ij}^x}{t_{ij}} \right) \frac{dt_{ij}^x}{d\theta_i^\alpha} + \left( \frac{t_{ij}^y}{t_{ij}} \right) \frac{dt_{ij}^y}{d\theta_i^\alpha} + \left( \frac{t_{ij}^z}{t_{ij}} \right) \frac{dt_{ij}^z}{d\theta_i^\alpha}. \quad (\text{A13})$$

With the help of Eqs. (A10) and (A11) we can solve the above two differential equations. As the tangential threshold is a linear function of overlap distance  $\delta_{ij}$  [see Eq. (A5)], it also gets modified due to a change in  $r_i^\alpha$  as

$$\frac{dt_{ij}^*}{dr_i^\alpha} = -\mu \left( \frac{k_n}{k_t} \right) \frac{r_{ij}^\alpha}{r_{ij}}, \quad (\text{A14})$$

and it is unaffected by the change in rotation,  $\frac{dt_{ij}^*}{d\theta_i^\alpha} = 0$ .

## APPENDIX B: EVALUATION OF $J$

### 1. Derivative of tangential force

The derivative of tangential force [Eq. (A4)] with respect to  $r_i^\alpha$  is

$$\begin{aligned} \frac{\partial F_{ij}^{(t)\beta}}{\partial r_i^\alpha} = & -k_t \frac{\partial}{\partial r_i^\alpha} \left[ \delta_{ij}^{1/2} (t_{ij}^\beta + \tilde{t} t_{ij}^\beta - \tilde{t}^2 t_{ij}^\beta) \right] \\ = & -\frac{1}{2} \delta_{ij}^{-1} \frac{r_{ij}^\alpha}{r_{ij}} F_{ij}^{(t)\beta} - k_t \delta_{ij}^{1/2} \left[ (1 + \tilde{t} - \tilde{t}^2) \frac{\partial t_{ij}^\beta}{\partial r_i^\alpha} \right. \\ & \left. + (\tilde{t}^\beta - 2\tilde{t}\tilde{t}^\beta) \frac{\partial t_{ij}}{\partial r_i^\alpha} + (-\tilde{t}\tilde{t}^\beta + 2\tilde{t}^2\tilde{t}^\beta) \frac{\partial t_{ij}^*}{\partial r_i^\alpha} \right]. \end{aligned} \quad (\text{B1})$$

Here we use the notation  $\tilde{t}$  to represent the ratio  $t_{ij}/t_{ij}^*$ , and the notation  $\tilde{t}^\beta$  for  $t_{ij}^\beta/t_{ij}^*$ . The expressions for all the three partial differentiation in (B1) are already shown in (A11), (A12), and (A14).

Similarly, the derivative of tangential force with respect to  $\theta_i^\alpha$  (using the same notation as above) can be found as

$$\frac{\partial F_{ij}^{(t)\beta}}{\partial \theta_i^\alpha} = -k_t \delta_{ij}^{1/2} \left[ (1 + \tilde{t} - \tilde{t}^2) \frac{\partial t_{ij}^\beta}{\partial \theta_i^\alpha} + (\tilde{t}^\beta - 2\tilde{t}\tilde{t}^\beta) \frac{\partial t_{ij}}{\partial \theta_i^\alpha} \right]. \quad (\text{B2})$$

From the above two equations it is then understood that if  $r_{ij}$  and  $t_{ij}$  are known, the differential equations can be solved easily. When  $\tilde{t}^\beta$  is negligible for all  $\beta$ , then  $\tilde{t} \approx 0$ . This translates to  $-k_t \delta_{ij}^{1/2} \frac{\partial t_{ij}^\beta}{\partial \theta_i^\alpha}$  implying that even in the case of zero tangential displacement and, therefore, zero tangential force, the above derivative can be finite.

### 2. Derivative of normal force

The derivative of normal force [Eq. (A3)] with respect to  $r_i^\alpha$  is

$$\begin{aligned} \frac{\partial F_{ij}^{(n)\beta}}{\partial r_i^\alpha} = & k_n \frac{\partial}{\partial r_i^\alpha} \left[ \delta_{ij}^{3/2} \frac{r_{ij}^\beta}{r_{ij}} \right] \\ = & k_n \delta_{ij}^{1/2} \left[ \Delta_{\alpha\beta} \frac{\delta_{ij}}{r_{ij}} - \frac{3}{2} \frac{r_{ij}^\alpha r_{ij}^\beta}{r_{ij}^2} - \left( \frac{\delta_{ij}}{r_{ij}} \right) \frac{r_{ij}^\alpha r_{ij}^\beta}{r_{ij}^2} \right], \end{aligned} \quad (\text{B3})$$

where  $\Delta_{\alpha\beta}$  is the Kronecker  $\delta$ . The derivative of total force, which reads

$$\frac{\partial F_{ij}^\beta}{\partial r_i^\alpha} = \frac{\partial F_{ij}^{(n)\beta}}{\partial r_i^\alpha} + \frac{\partial F_{ij}^{(t)\beta}}{\partial r_i^\alpha}, \quad (\text{B4})$$

$$\frac{\partial F_{ij}^\beta}{\partial \theta_i^\alpha} = \frac{\partial F_{ij}^{(t)\beta}}{\partial \theta_i^\alpha}, \quad (\text{B5})$$

can be solved using (B3), (B1), and (B2).

### 3. Derivative of torque

The torque of particle  $j$  due to tangential force  $\mathbf{F}^{(t)}_{ij}$  is  $\mathbf{T}_j = -\sigma_j (\hat{\mathbf{r}}_{ij} \times \mathbf{F}^{(t)}_{ij}) \equiv \sigma_j \tilde{\mathbf{T}}_j$ . In three dimensions, the

components of  $\tilde{T}_{ij}$  are

$$\begin{aligned}\tilde{T}_{ij}^x &= -\left[\left(\frac{y_{ij}}{r_{ij}}\right)F_{ij}^{(t)z} - \left(\frac{z_{ij}}{r_{ij}}\right)F_{ij}^{(t)y}\right], \\ \tilde{T}_{ij}^y &= -\left[\left(\frac{z_{ij}}{r_{ij}}\right)F_{ij}^{(t)x} - \left(\frac{x_{ij}}{r_{ij}}\right)F_{ij}^{(t)z}\right], \\ \tilde{T}_{ij}^z &= -\left[\left(\frac{x_{ij}}{r_{ij}}\right)F_{ij}^{(t)y} - \left(\frac{y_{ij}}{r_{ij}}\right)F_{ij}^{(t)x}\right].\end{aligned}\quad (\text{B6})$$

The derivatives of  $\tilde{T}_{ij}^x$ ,  $\tilde{T}_{ij}^y$ ,  $\tilde{T}_{ij}^z$  then are

$$\begin{aligned}\frac{\partial \tilde{T}_{ij}^x}{\partial r_i^\alpha} &= -\left(\frac{\delta_{\alpha y}}{r_{ij}} - \frac{y_{ij}r_{ij}^\alpha}{r_{ij}^3}\right)F_{ij}^{(t)z} - \left(\frac{y_{ij}}{r_{ij}}\right)\frac{\partial F_{ij}^{(t)z}}{\partial r_i^\alpha} + \left(\frac{\delta_{\alpha z}}{r_{ij}} - \frac{z_{ij}r_{ij}^\alpha}{r_{ij}^3}\right)F_{ij}^{(t)y} + \left(\frac{z_{ij}}{r_{ij}}\right)\frac{\partial F_{ij}^{(t)y}}{\partial r_i^\alpha}, \\ \frac{\partial \tilde{T}_{ij}^y}{\partial r_i^\alpha} &= -\left(\frac{\delta_{\alpha z}}{r_{ij}} - \frac{z_{ij}r_{ij}^\alpha}{r_{ij}^3}\right)F_{ij}^{(t)x} - \left(\frac{z_{ij}}{r_{ij}}\right)\frac{\partial F_{ij}^{(t)x}}{\partial r_i^\alpha} + \left(\frac{\delta_{\alpha x}}{r_{ij}} - \frac{x_{ij}r_{ij}^\alpha}{r_{ij}^3}\right)F_{ij}^{(t)z} + \left(\frac{x_{ij}}{r_{ij}}\right)\frac{\partial F_{ij}^{(t)z}}{\partial r_i^\alpha}, \\ \frac{\partial \tilde{T}_{ij}^z}{\partial r_i^\alpha} &= -\left(\frac{\delta_{\alpha x}}{r_{ij}} - \frac{x_{ij}r_{ij}^\alpha}{r_{ij}^3}\right)F_{ij}^{(t)y} - \left(\frac{x_{ij}}{r_{ij}}\right)\frac{\partial F_{ij}^{(t)y}}{\partial r_i^\alpha} + \left(\frac{\delta_{\alpha y}}{r_{ij}} - \frac{y_{ij}r_{ij}^\alpha}{r_{ij}^3}\right)F_{ij}^{(t)x} + \left(\frac{y_{ij}}{r_{ij}}\right)\frac{\partial F_{ij}^{(t)x}}{\partial r_i^\alpha},\end{aligned}\quad (\text{B7})$$

where  $\delta_{\alpha x}$  (similarly,  $\delta_{\alpha y}$  and  $\delta_{\alpha z}$ ) is the Kronecker  $\delta$ , such that  $\delta_{xx} = 1$ ,  $\delta_{yx} = 0$ , and  $\delta_{zx} = 0$ , and

$$\begin{aligned}\frac{\partial \tilde{T}_{ij}^x}{\partial \theta_i^\alpha} &= -\left[\left(\frac{y_{ij}}{r_{ij}}\right)\frac{\partial F_{ij}^{(t)z}}{\partial \theta_i^\alpha} - \left(\frac{z_{ij}}{r_{ij}}\right)\frac{\partial F_{ij}^{(t)y}}{\partial \theta_i^\alpha}\right], \\ \frac{\partial \tilde{T}_{ij}^y}{\partial \theta_i^\alpha} &= -\left[\left(\frac{z_{ij}}{r_{ij}}\right)\frac{\partial F_{ij}^{(t)x}}{\partial \theta_i^\alpha} - \left(\frac{x_{ij}}{r_{ij}}\right)\frac{\partial F_{ij}^{(t)z}}{\partial \theta_i^\alpha}\right], \\ \frac{\partial \tilde{T}_{ij}^z}{\partial \theta_i^\alpha} &= -\left[\left(\frac{x_{ij}}{r_{ij}}\right)\frac{\partial F_{ij}^{(t)y}}{\partial \theta_i^\alpha} - \left(\frac{y_{ij}}{r_{ij}}\right)\frac{\partial F_{ij}^{(t)x}}{\partial \theta_i^\alpha}\right].\end{aligned}\quad (\text{B8})$$

The above two differential equations can be solved using (B1), and (B2).

#### 4. Jacobian

The dimension of Jacobian operator  $\mathbf{J}$  is force over length. To be consistent with the dimension we redefine the torque  $T$  and rotational coordinate  $\theta$  as

$$\tilde{T}_i = \frac{T_i}{\sigma_i}, \quad \text{and} \quad \tilde{\theta}_i = \sigma_i \theta_i. \quad (\text{B9})$$

In addition, the dynamic matrix has a contribution from the moment of inertia  $I_i = I_0 m_i \sigma_i^2$  as  $\Delta \omega_i = \mathbf{T}_i / I_i \Delta t$ . In our calculation, we assume that mass  $m_i$  and  $I_0$  both are one. The remaining contribution of  $I_i$ ,  $\sigma_i^2$ , is taken care of by rescaling the torque and the angular displacement as  $\tilde{T}_i$  and  $\tilde{\theta}_i$  (B9). For  $I_0 \neq 1$ , the contribution of  $I_0$  can be correctly anticipated if we rewrite (A7) as

$$\frac{d\mathbf{t}_{ij}}{dt} = \mathbf{v}_{ij} - \mathbf{v}_{ij}^n + \frac{1}{I_0} \hat{r}_{ij} \times (\sigma_i \boldsymbol{\omega}_i + \sigma_j \boldsymbol{\omega}_j) \quad (\text{B10})$$

$\mathbf{J}$  essentially contains four different derivatives:

*First type:* Derivative of force with respect to the position of particles:

$$A_{ij}^{\alpha\beta} = \sum_{k=0; k \neq j}^{N-1} \frac{\partial F_{kj}^\beta}{\partial r_i^\alpha} = \frac{\partial F_{ij}^\beta}{\partial r_i^\alpha}, \quad \text{for } i \neq j,$$

$$A_{ii}^{\alpha\beta} = \sum_{j=0; j \neq i}^{N-1} \frac{\partial F_{ji}^\beta}{\partial r_i^\alpha} = - \sum_{j=0; j \neq i}^{N-1} A_{ij}^{\alpha\beta}, \quad (\text{B11})$$

where  $N$  is the total number of particles.  $A_{ij}^{\alpha\beta}$  is symmetric if we change pairs,  $A_{ij}^{\alpha\beta} = A_{ji}^{\alpha\beta}$ ; however, the symmetry is not guaranteed with the interchange of  $\alpha$  and  $\beta$ .

*Second type:* Derivative of force with respect to rotational coordinate:

$$\begin{aligned}C_{ij}^{\alpha\beta} &= - \sum_{k=0; k \neq j}^{N-1} \frac{\partial F_{kj}^\beta}{\partial \tilde{\theta}_i^\alpha} = - \frac{\partial F_{ij}^\beta}{\partial \tilde{\theta}_i^\alpha}, \quad \text{for } i \neq j, \\ C_{ii}^{\alpha\beta} &= - \sum_{j=0; j \neq i}^{N-1} \frac{\partial F_{ji}^\beta}{\partial \tilde{\theta}_i^\alpha} = - \sum_{j=0; j \neq i}^{N-1} C_{ij}^{\alpha\beta}.\end{aligned}\quad (\text{B12})$$

The negative sign ensures that in stable systems all the eigenvalues are positive.  $C_{ij}^{\alpha\beta}$  is asymmetric:  $C_{ij}^{\alpha\beta} = -C_{ji}^{\alpha\beta}$ .

*Third type:* Derivative of torque with respect to position:

$$\begin{aligned}B_{ij}^{\alpha\beta} &= \sum_{k=0; k \neq j}^{N-1} \frac{\partial \tilde{T}_{kj}^\beta}{\partial r_i^\alpha} = \frac{\partial \tilde{T}_j^\beta}{\partial r_i^\alpha}, \quad \text{for } i \neq j, \\ B_{ii}^{\alpha\beta} &= \sum_{j=0; j \neq i}^{N-1} \frac{\partial \tilde{T}_{ji}^\beta}{\partial r_i^\alpha} = \sum_{j=0; j \neq i}^{N-1} B_{ij}^{\alpha\beta}.\end{aligned}\quad (\text{B13})$$

$B_{ij}^{\alpha\beta}$  is also asymmetric:  $B_{ij}^{\alpha\beta} = -B_{ji}^{\alpha\beta}$ .

*Fourth type:* Derivative of torque with respect to rotational coordinate:

$$\begin{aligned}D_{ij}^{\alpha\beta} &= - \sum_{k=0; k \neq j}^{N-1} \frac{\partial \tilde{T}_{kj}^\beta}{\partial \tilde{\theta}_i^\alpha} = - \frac{\partial \tilde{T}_j^\beta}{\partial \tilde{\theta}_i^\alpha}, \quad \text{for } i \neq j, \\ D\alpha\beta_{ii} &= - \sum_{j=0; j \neq i}^{N-1} \frac{\partial \tilde{T}_{ji}^\beta}{\partial \tilde{\theta}_i^\alpha} = \sum_{j=0; j \neq i}^{N-1} D_{ij}^{\alpha\beta}.\end{aligned}\quad (\text{B14})$$

The negative sign ensures that in stable systems all the eigenvalues are positive.  $D_{ij}^{\alpha\beta}$  is symmetric:  $D_{ij}^{\alpha\beta} = D_{ji}^{\alpha\beta}$ .

### 5. Arrangement of Jacobian matrix

All the  $J$ -matrix elements are combined with the following arrangement:

$$\mathbf{J} = \left[ \begin{array}{ccc|ccc} \frac{\partial F_x}{\partial x} & \frac{\partial F_y}{\partial x} & \frac{\partial F_z}{\partial x} & \frac{\partial \tilde{T}_x}{\partial x} & \frac{\partial \tilde{T}_y}{\partial x} & \frac{\partial \tilde{T}_z}{\partial x} \\ \frac{\partial F_x}{\partial y} & \frac{\partial F_y}{\partial y} & \frac{\partial F_z}{\partial y} & \frac{\partial \tilde{T}_x}{\partial y} & \frac{\partial \tilde{T}_y}{\partial y} & \frac{\partial \tilde{T}_z}{\partial y} \\ \frac{\partial F_x}{\partial z} & \frac{\partial F_y}{\partial z} & \frac{\partial F_z}{\partial z} & \frac{\partial \tilde{T}_x}{\partial z} & \frac{\partial \tilde{T}_y}{\partial z} & \frac{\partial \tilde{T}_z}{\partial z} \\ \hline \frac{\partial F_x}{\partial \theta_x} & \frac{\partial F_y}{\partial \theta_x} & \frac{\partial F_z}{\partial \theta_x} & \frac{\partial \tilde{T}_x}{\partial \theta_x} & \frac{\partial \tilde{T}_y}{\partial \theta_x} & \frac{\partial \tilde{T}_z}{\partial \theta_x} \\ \frac{\partial F_x}{\partial \theta_y} & \frac{\partial F_y}{\partial \theta_y} & \frac{\partial F_z}{\partial \theta_y} & \frac{\partial \tilde{T}_x}{\partial \theta_y} & \frac{\partial \tilde{T}_y}{\partial \theta_y} & \frac{\partial \tilde{T}_z}{\partial \theta_y} \\ \frac{\partial F_x}{\partial \theta_z} & \frac{\partial F_y}{\partial \theta_z} & \frac{\partial F_z}{\partial \theta_z} & \frac{\partial \tilde{T}_x}{\partial \theta_z} & \frac{\partial \tilde{T}_y}{\partial \theta_z} & \frac{\partial \tilde{T}_z}{\partial \theta_z} \end{array} \right] = \left[ \begin{array}{c|c} \mathbf{A} & \mathbf{B} \\ \mathbf{C} & \mathbf{D} \end{array} \right]. \quad (\text{B15})$$

Every element of the above  $J$ -matrix is expanded into  $N \times N$  subelements corresponding to  $i$ - $j$  particle pairs. The total size of the matrix for  $D = 3$  is therefore  $(2D)N \times (2D)N$ .

- 
- [1] A. Liu and S. Nagel, *Nature (London)* **396**, 21 (1998).
- [2] C. S. O'Hern, S. A. Langer, A. J. Liu, and S. R. Nagel, *Phys. Rev. Lett.* **86**, 111 (2001).
- [3] M. E. Cates, J. P. Wittmer, J.-P. Bouchaud, and P. Claudin, *Phys. Rev. Lett.* **81**, 1841 (1998).
- [4] T. S. Majmudar, M. Sperl, S. Luding, and R. P. Behringer, *Phys. Rev. Lett.* **98**, 058001 (2007).
- [5] H. Masuda, K. Higashitani, and H. Yoshida, *Powder Technology Handbook* (CRC Press, Boca Raton, FL, 2006).
- [6] J. Chattoraj, O. Gendelman, M. Pica Ciamarra, and I. Procaccia, *Phys. Rev. Lett.* **123**, 098003 (2019).
- [7] J. Chattoraj, O. Gendelman, M. P. Ciamarra, and I. Procaccia, *Phys. Rev. E* **100**, 042901 (2019).
- [8] H. Charan, J. Chattoraj, M. P. Ciamarra, and I. Procaccia, *Phys. Rev. Lett.* **124**, 030602 (2020).
- [9] R. D. Mindlin, *J. Appl. Mech.*, ASME **16**, 259 (1949).
- [10] S. Plimpton, *J. Comput. Phys.* **117**, 1 (1995).
- [11] I. Agnolin and J.-N. Roux, *Phys. Rev. E* **76**, 061304 (2007).
- [12] P. A. Johnson and X. Jia, *Nature (London)* **437**, 871 (2005).
- [13] C. Marone, *Annu. Rev. Earth Planet Sci.* **26**, 643 (1998).
- [14] P. Johnson, B. Ferdowsi, B. Kaproth, M. Scuderi, M. Griffa, J. Carmeliet, R. Guyer, P.-Y. Le Bas, D. Trugman, and C. Marone, *Geophys. Res. Lett.* **40**, 5627 (2013).